

# Nonconvex Distributed Optimization Based Power Allocation for Maximizing DL-UL Total Sum Rate in Dynamic TDD Systems

Jin-Xin Kong, Shaoshi Yang, *Senior Member, IEEE*, and Sheng Chen, *Life Fellow, IEEE*

**Abstract**—We investigate the power allocation problem of a dynamic time division duplexing based heterogeneous network comprising downlink (DL) macro base stations (MBSs) and uplink (UL) small base stations (SBSs). In such networks, beyond intra-cell interference, the asynchronous DL transmission of MBSs and UL transmission of SBSs introduce additional interference known as cross-link interference. This interference occurs not only between MBSs and SBSs, but also between macro-cell user equipment and small-cell user equipment (SUE). To maximize the sum rate of UL and DL, we formulate a non-convex distributed optimization problem where power allocation variables of both DL and UL are to be optimized. We propose a power allocation algorithm relying on the Lagrange method with logarithmic barrier. Simulation results demonstrate that our proposed algorithm outperforms the representative benchmark schemes.

**Index Terms**—Power allocation, cross-link interference, dynamic TDD, interference mitigation.

## I. INTRODUCTION

**D**YNAMIC Time Division Duplexing (D-TDD) enhances spectral efficiency in future mobile networks by dynamically reallocating time slots between uplink (UL) and downlink (DL) transmissions. This adaptability accommodates the coexistence of macro and small base stations (MBSs and SBSs) and balances asymmetric UL and DL traffic in dense heterogeneous networks. However, it can result in cross-link interference (CLI) as adjacent cells may operate in different transmission directions simultaneously, posing a challenge for interference management. According to [1], various CLI mitigation schemes for D-TDD systems can be categorized into the following approaches: 1) clustering; 2) scheduling and resource allocation; 3) power control; 4) beamforming; 5) UL/DL configuration; 6) joint optimization of coordination-based schemes. Our research focuses on the power control, which adjusts transmission power to increase the desired signal power or reduce the interference power. This approach is crucial as it directly impacts the performance of both the UL and DL.

This work was supported by Beijing Municipal Natural Science Foundation under Grant L242013.

J.-X. Kong and S. Yang (*Corresponding author*) are with the School of Information and Communication Engineering, Beijing University of Posts and Telecommunications, with the Key Laboratory of Universal Wireless Communications, Ministry of Education, and also with the Key Laboratory of Mathematics and Information Networks, Ministry of Education, Beijing 100876, China (e-mails: shaoshi.yang@bupt.edu.cn, kongjinxin@bupt.edu.cn).

S. Chen is with the School of Electronics and Computer Science, University of Southampton, Southampton SO17 1BJ, U.K. (e-mail: sqc@ecs.soton.ac.uk).

## A. Related Works

In the existing literature, power control schemes for D-TDD systems can be categorized based on the directions of signal transmission, namely, UL, DL, or bidirectional UL-DL.

UL power control is mainly to resist BS interference. BS can adjust the power of UEs on UL to reduce UE interference to adjacent cells [2], or improve UL performance when there is BS interference from adjacent cells [3]. The work [4] proposed an UL power control algorithm based on interference contribution rate (ICR) to mitigate interference problems in heterogeneous networks.

The DL power control is also vital. The work [5] reviewed a variety of CLI mitigation options, including adjusting DL transmission power through a simple reinforcement learning (RL) algorithm. The study [6] explored reducing interference in local 5G networks to enhance the viability of micro operator deployments. The work [7] discussed the CLI mitigation technology in 5G new radio TDD system, focusing on the DL power control scheme.

Additionally, some studies have focused on mitigating CLI in D-TDD systems by controlling simultaneously the transmission power on both UL and DL. The multi-agent deep reinforcement learning (MADRL) method is used to adjust power allocation in [8], so as to effectively manage CLI between cells.

In the landscape of research aimed at mitigating CLI through power control, two fundamental mechanisms have emerged: 1) diminishing the DL transmission power of base stations (BSs), and 2) amplifying the UL transmission power of user equipments (UEs). The former strategy effectively reduces CLI in adjacent cells, while the latter bolsters the reception of essential UL signals amidst interference from neighboring cells. However, these approaches are not operational without trade-offs. Diminishing transmission power can attenuate the signal strength of the desired signal on the DL, and increasing it can exacerbate CLI. The existing power control paradigms have yet to reconcile this delicate balance between interference mitigation and system performance optimization. The challenge of judiciously distributing UL and DL transmission power to mitigate CLI while enhancing overall system performance remains an open question in the field.

## B. Our Contributions

This paper confronts the aforementioned challenge of power allocation in D-TDD heterogeneous networks. Our focus is on

reconciling the competing demands of interference mitigation and system performance optimization, specifically by reducing interference between BSs and UEs while maximizing the total sum rate. To this end, we propose an innovative optimization framework that aims to maximize the sum rate of both UL and DL by strategically allocating transmission power across the multi-antennas of MBSs and the single-antenna of UEs—a novel approach not explored in prior studies.

The optimization problem we formulate is inherently non-convex and distributed in nature, posing significant mathematical challenges. Such problems lack universal solutions and are typically addressed using heuristic algorithms, such as simulated annealing (SA) and particle swarm optimization (PSO). These heuristic methods come with their limitations – they are prone to converging on local optima rather than the global optimum due to their incremental nature, and their efficacy is heavily dependent on the selection of parameters and initial conditions, which often requires empirical tuning. To surmount these obstacles, we introduce an iterative, nonconvex distributed optimization methodology. Our key contributions are outlined as follows.

- In order to mitigate CLI while optimizing the total sum rate, we formulate the UL-DL power allocation problem as an optimization problem that maximizes the sum rate of UL and DL.
- For solving this challenging nonconvex distributed optimization problem, we propose a mathematical optimization method based on the Lagrange method with logarithmic barrier (LMLB). We further discuss the computational complexity and the convergence behavior of the proposed algorithm and the impact of initial values.
- We assess the proposed algorithm's performance in terms of the system's total sum rate, power allocation and interference management. Simulation results demonstrate the superiority and effectiveness of our algorithm.

## II. SYSTEM MODEL AND PROBLEM FORMULATION

We consider a D-TDD based wireless network consisting of multiple BSs and their respective UEs. Here the BS is a generic term, which can represent an MBS, an SBS, or a Wi-Fi access point (AP). Without loss of generality, our exposition will be based on a two-BS system model, as shown in Fig. 1. We assume that the transmission direction in the macro cell is DL, i.e., the signal is transmitted from the MBS to the macro cell UEs (MUEs), and the transmission direction in the small cell is UL, i.e., the signal is transmitted to the SBS from the small cell UEs (SUEs). The numbers of active UEs in the macro cell and the small cell are  $K$  and  $L$ , respectively. The MBS has  $M$  antennas, the SBS has  $N$  antennas, and each UE is equipped with a single antenna. The received signal at the  $k$ th MUE can be expressed as

$$y_k^{\text{DL}} = \left(\mathbf{h}_k^{\text{DL}}\right)^{\text{T}} \mathbf{w}_k^{\text{DL}} s_k^{\text{DL}} + \left(\mathbf{h}_k^{\text{DL}}\right)^{\text{T}} \sum_{i \in \Phi_k \setminus k} \mathbf{w}_i^{\text{DL}} s_i^{\text{DL}} + \sum_{l \in \Psi_k} h_{l,k} \sqrt{p_l^{\text{UL}}} s_l^{\text{UL}} + n_k, \quad (1)$$

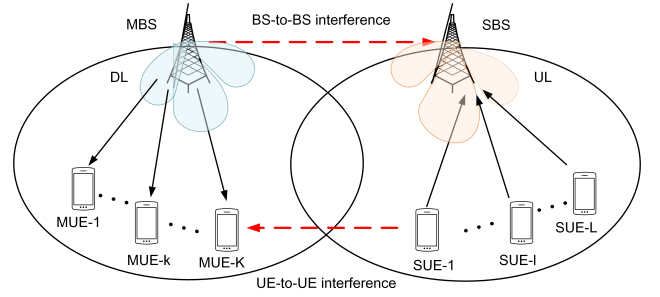


Fig. 1. System model.

where  $\mathbf{h}_k^{\text{DL}} \in \mathbb{C}^{M \times 1}$  is the DL channel state information (CSI) vector linking the MBS to the  $k$ th MUE,  $s_k^{\text{DL}} \in \mathbb{C}$  with  $|s_k^{\text{DL}}|^2 = 1$  is the symbol transmitted from the MBS to the  $k$ th MUE,  $s_l^{\text{UL}} \in \mathbb{C}$  with  $|s_l^{\text{UL}}|^2 = 1$  is the symbol transmitted from the  $l$ th SUE to the SBS, and  $h_{l,k} \in \mathbb{C}$  is the CSI coefficient linking the  $l$ th SUE to the  $k$ th MUE, while  $p_l^{\text{UL}} \in \mathbb{R}$  is the power allocated by the SBS to the  $l$ th SUE, and  $\mathbf{w}_i^{\text{DL}} \in \mathbb{R}^{M \times 1}$  is the DL power allocation vector given by

$$\mathbf{w}_i^{\text{DL}} = \left[ \sqrt{p_{1,i}^{\text{DL}}}, \dots, \sqrt{p_{m,i}^{\text{DL}}}, \dots, \sqrt{p_{M,i}^{\text{DL}}} \right]^{\text{T}}, i \in \Phi_k, \quad (2)$$

in which  $p_{m,i}^{\text{DL}}$  is the power allocated to the symbol  $s_i^{\text{DL}}$  on the  $m$ th antenna of the MBS. Additionally,  $\Phi_k$  denotes the set of MUEs occupying the same time-frequency resource blocks (RBs) as the  $k$ th MUE, hence  $|\Phi_k| = K$ , and  $\Psi_k$  is the set of SUEs occupying the same RBs as the  $k$ th MUE, hence  $|\Psi_k| = L$ . Finally,  $n_k \sim \mathcal{CN}(0, \sigma^2)$  represents the additive white Gaussian noise (AWGN) at the  $k$ th MUE.

Then, the SINR at the  $k$ th MUE receiver is given by

$$\text{SINR}_k^{\text{DL}} = \frac{\|\mathbf{h}_k^{\text{DL}} \mathbf{w}_k^{\text{DL}}\|^2}{\varphi_k + \psi_k + \sigma^2}, \quad (3)$$

where the inter-user interference (IUI) inside the serving macro cell and the CLI from the neighbouring small cell are given by

$$\varphi_k = \sum_{i \in \Phi_k \setminus k} \|\mathbf{h}_k^{\text{DL}} \mathbf{w}_i^{\text{DL}}\|^2, \quad (4)$$

$$\psi_k = \sum_{l \in \Psi_k} |h_{l,k}|^2 p_l^{\text{UL}}, \quad (5)$$

respectively. Upon assuming that idealized transceivers operating at the Shannon capacity are employed, the DL sum rate of the macro cell is given by

$$R^{\text{DL}} = \sum_{k=1}^K R_k^{\text{DL}} = \sum_{k=1}^K B_k \log_2 \left( 1 + \frac{\|\mathbf{h}_k^{\text{DL}} \mathbf{w}_k^{\text{DL}}\|^2}{\varphi_k + \psi_k + \sigma^2} \right), \quad (6)$$

where  $B_k$  is the bandwidth allocated to the  $k$ th MUE.

On the other hand, the signal received by the SBS with the  $l$ th SUE as the target UE is expressed as

$$\mathbf{y}_l^{\text{UL}} = \mathbf{h}_l^{\text{UL}} \sqrt{p_l^{\text{UL}}} s_l^{\text{UL}} + \sum_{i \in \Psi_l \setminus l} \mathbf{h}_i^{\text{UL}} \sqrt{p_i^{\text{UL}}} s_i^{\text{UL}} + \mathbf{H}^{\text{BS}} \mathbf{W}^{\text{DL}} \mathbf{s}^{\text{DL}} + \mathbf{n}, \quad (7)$$

where  $\mathbf{h}_l^{\text{UL}} \in \mathbb{C}^{N \times 1}$  is the CSI vector from the  $l$ th SUE to the SBS,  $\mathbf{H}^{\text{BS}} \in \mathbb{C}^{N \times M}$  is the CSI matrix from the MBS to the SBS,  $\mathbf{W}^{\text{DL}} = [\mathbf{w}_1^{\text{DL}}, \mathbf{w}_2^{\text{DL}}, \dots, \mathbf{w}_K^{\text{DL}}] \in \mathbb{R}^{M \times K}$ , and  $\mathbf{s}^{\text{DL}} = [s_1^{\text{DL}}, s_2^{\text{DL}}, \dots, s_K^{\text{DL}}]^T \in \mathbb{C}^{K \times 1}$ , while  $\mathbf{n} \in \mathbb{C}^{N \times 1}$  is the AWGN vector, whose entries obey  $\mathcal{CN}(0, \sigma^2)$ .

Hence, when the  $l$ th SUE is the target UE, the SINR at the SBS is given by

$$\text{SINR}_l^{\text{UL}} = \frac{\|\mathbf{h}_l^{\text{UL}}\|^2 p_l^{\text{UL}}}{\varphi_l + \psi_l + \sigma^2}, \quad (8)$$

where the IUI inside the serving small cell and the CLI from the neighbouring macro cell are given by

$$\varphi_l = \sum_{i \in \Psi_l \setminus l} \|\mathbf{h}_i^{\text{UL}}\|^2 p_i^{\text{UL}}, \quad (9)$$

$$\psi_l = \|\mathbf{H}^{\text{BS}} \mathbf{W}^{\text{DL}} \mathbf{s}^{\text{DL}}\|^2, \quad (10)$$

respectively. Then the capacity-achieving UL sum rate of the small cell is given by

$$R^{\text{UL}} = \sum_{l=1}^L R_l^{\text{UL}} = \sum_{l=1}^L B_l \log_2 \left( 1 + \frac{\|\mathbf{h}_l^{\text{UL}}\|^2 p_l^{\text{UL}}}{\psi_l + \varphi_l + \sigma^2} \right), \quad (11)$$

where  $B_l$  is the bandwidth allocated to the  $l$ th SUE.

Our goal is to maximize the sum rate of DL and UL by properly allocating power. This involves the DL transmission power on each antenna of the MBS and the UL transmission power of each SUE. This optimization problem can be formulated as

$$\max_{\{p_l^{\text{UL}}\}_{l=1}^L, \{\mathbf{w}_k^{\text{DL}}\}_{k=1}^K} R^{\text{DL}} + R^{\text{UL}}, \quad (12a)$$

$$\text{s.t.} \quad \sum_{k=1}^K \text{Tr} [\mathbf{w}_k^{\text{DL}} (\mathbf{w}_k^{\text{DL}})^T] \leq P_{\max}^{\text{DL}}, \quad (12b)$$

$$p_l^{\text{UL}} \leq P_{l, \max}^{\text{UL}}, l = 1, 2, \dots, L, \quad (12c)$$

$$R_k^{\text{DL}} \geq R_{k, \min}^{\text{DL}}, k = 1, 2, \dots, K, \quad (12d)$$

$$R_l^{\text{UL}} \geq R_{l, \min}^{\text{UL}}, l = 1, 2, \dots, L. \quad (12e)$$

Constraint (12b) imposes the maximum transmission power on the MBS, and (12c) sets the maximum transmission power to each SUE by the SBS, while (12d) and (12e) impose the minimum achievable rates for each MUE and SUE, respectively.

We have the following observations for the above optimization problem. 1) To increase  $R^{\text{DL}}$ , intuitively we increase the values of  $\{\mathbf{w}_k^{\text{DL}}\}$ . This action improves the DL rate for the MUEs. However, it also strengthens the CLI imposed on the UL transmission of the neighbouring small cell. Similar observation can also be made for the UL. 2) The objective function (12a) is non-concave, so (12) is a challenging nonconvex optimization problem that needs to be solved in a distributed manner involving different types of network nodes.

### III. PROPOSED POWER ALLOCATION ALGORITHM

In order to solve the challenging nonconvex distributed optimization problem (12), we propose a mathematical optimization algorithm designed to tackle common challenges encountered by traditional heuristic algorithms, and we analyze the convergence and complexity of the algorithm.

#### A. Optimization algorithm with logarithmic barrier

To address the nonconvex distributed optimization problem formulated, in this subsection we will introduce the proposed LMLB. The optimization problem (12) can be expressed in the following form:

$$\begin{aligned} \min \quad & f(\mathbf{x}) \\ \text{s.t.} \quad & g_i(\mathbf{x}) \leq 0, \quad i = 1, 2, \dots, m, \end{aligned} \quad (13)$$

where  $\mathbf{x}$  represents a vector.

First, we incorporate the inequality constraints into the objective function by employing the barrier function  $B(x)$ , and transform (13) as follows:

$$\min \quad f(\mathbf{x}) + \mu B(\mathbf{x}), \quad (14)$$

where  $\mu$  represents a positive barrier parameter. Let  $\mathcal{L}_B(\mathbf{x}, \mu) = f(\mathbf{x}) + \mu B(\mathbf{x})$ , and refer to it as the Lagrangian function with a barrier term. We define the logarithmic barrier function on the set of interior points  $\mathbb{S}$  as follows:

$$B(\mathbf{x}) = - \sum_{i=1}^m \log(-g_i(\mathbf{x})). \quad (15)$$

Furthermore, for the barrier parameter sequence  $\{\mu^{(k)}\}$ , we obtain the following corresponding unconstrained minimization problems:

$$\begin{aligned} \mathbf{x}^{(k)} &= \arg \min_{\mathbf{x} \in \mathbb{S}} \mathcal{L}_B(\mathbf{x}, \mu^{(k)}) \\ &= \arg \min_{\mathbf{x} \in \mathbb{S}} \left\{ f(\mathbf{x}) - \sum_{i=1}^m \mu^{(k)} \log(-g_i(\mathbf{x})) \right\}. \end{aligned} \quad (16)$$

Now, we present the following theorem concerning the sequence  $\{\mathbf{x}^{(k)}\}$  and the optimal solution of (13).

*Theorem 3.1:* If for all  $k$ ,  $0 < \mu^{(k)} < \mu^{(k+1)}$ , and  $\mu^{(k)} \rightarrow 0$ , assuming that any feasible point can be arbitrarily approached by a vector within  $\mathbb{S}$ , then the limit point of the sequence  $\{\mathbf{x}^{(k)}\}$  is the global optimal solution of (13).

*Proof:* See [10].

Obviously,  $\mathbf{x}^{(k)}$  serves as an approximation to the optimal solution of (13), converging to the optimal solution only when  $\mu^{(k)} \rightarrow 0$ . The following theorem quantifies the degree of approximation.

*Theorem 3.2:* The approximate optimal value of the objective function at the solution of (16) is within an error of  $m\mu^{(k)}$  compared to the optimal value of (13).

*Proof:* See [11].

The above theorems have proven that by solving (16), we can obtain the suboptimal solution to (13), which approximates the optimal value of (13) with an error not greater than  $m\mu^{(k)}$ . Additionally, the approximation accuracy increases as the  $\mu^{(k)}$  decreases. The sequential unconstrained minimization technique (SUMT) in [10] provides a scheme for iteratively reducing the sequence  $\{\mu^{(k)}\}$ . The specific steps are shown in Algorithm 1.

The problem now becomes how to solve (16). To ensure that the iterative sequence remains within  $\mathbb{S}$ , we employ an

---

**Algorithm 1** SUMT

---

**Require:** feasible point  $\mathbf{x}^{(0)}$ , initial value  $\mu > 0$ , error threshold  $\epsilon > 0$ , scaling factor  $0 < \theta < 1$ .

- 1: **while** True **do**
- 2:   starting from  $\mathbf{x}^{(0)}$ , solve (16) to obtain  $\mathbf{x}(\mu)$
- 3:   update  $\mathbf{x}^{(0)} := \mathbf{x}(\mu)$
- 4:   **if**  $m\mu < \epsilon$  **then**
- 5:     break the loop
- 6:   **end if**
- 7:   update  $\mu := \theta\mu$
- 8: **end while**

---

improved Newton descent method and update the variables according to the following rule:

$$\mathbf{x}^{(k+1)} = \mathbf{x}^{(k)} + \alpha^{(k)} \mathbf{d}^{(k)}, \quad (17)$$

where  $\alpha^{(k)}$  is the step size determined by the Armijo criterion for the  $k$ th iteration. The search direction  $\mathbf{d}^{(k)}$  is determined by the following linear system:

$$\left( \nabla^2 \mathcal{L}_B(\mathbf{x}^{(k)}) + \Delta^{(k)} \right) \mathbf{d}^{(k)} = -\nabla \mathcal{L}_B(\mathbf{x}^{(k)}), \quad (18)$$

where  $\Delta^{(k)}$  is a diagonal matrix that ensures positive definiteness of  $\nabla^2 \mathcal{L}_B(\mathbf{x}^{(k)}) + \Delta^{(k)}$ . Since  $f(\mathbf{x})$  is a nonconvex function, its Hessian matrix may not be positive definite, and thus it requires diagonal modification to make sure  $\mathbf{d}^{(k)}$  a direction of descent.

Subsequently, the Cholesky decomposition is used to factorize this positive definite matrix and solve (18) to determine the search direction:

$$\mathbf{L}\mathbf{L}' = \nabla^2 \mathcal{L}_B(\mathbf{x}^{(k)}) + \Delta^{(k)}, \quad (19)$$

where  $\mathbf{L}$  is the lower triangular matrix obtained from the Cholesky decomposition of the corrected Hessian matrix.

Typically, unconstrained minimization methods are terminated when the gradient of the objective function is sufficiently small rather than strictly equal to zero [11]. We refer to the following inequality as the stopping criterion for the iteration:

$$\frac{\|\nabla \mathcal{L}_B(\mathbf{x}^{(k)})\|_2}{\|\nabla \mathcal{L}_B(\mathbf{x}^{(0)})\|_2} \leq \varepsilon, \quad (20)$$

where  $\varepsilon$  is a small positive scalar.

The LMLB algorithm builds upon SUMT, by first using the improved Newton descent method to obtain the solution to (16) corresponding to the initial value  $\mu$ . This solution then serves as the starting point for the next unconstrained minimization problem, and  $\mu$  is updated to further approximate, continuing until the error is reduced to an acceptable level. The complete algorithmic procedure is shown in Algorithm 2.

### B. Algorithm complexity

The convergence analysis of LMLB is straightforward. By employing the improved Newton descent method to solve (16), when the initial barrier parameter  $\mu^{(0)}$  has been iteratively reduced  $k$  times, the solution to (16) is a suboptimal solution

---

**Algorithm 2** The Proposed LMLB Algorithm

---

**Require:** objective function, constraint functions, feasible point  $\mathbf{x}^{(0)}$ , initial value  $\mu > 0$ , error threshold  $\epsilon > 0$ , stop criterion scalar  $\varepsilon > 0$ , scaling factor  $0 < \theta < 1$ .

**Ensure:**  $R_{l_{\max}}$ ,  $\mathbf{x}_{\text{best}}$ .

- 1: **while**  $m/\mu \geq \epsilon$  **do**
- 2:   **while** True **do**
- 3:     calculate  $\nabla \mathcal{L}_B(\mathbf{x}^{(k)})$ ,  $\nabla^2 \mathcal{L}_B(\mathbf{x}^{(k)})$
- 4:     calculate  $\alpha^{(k)}$  by Armijo criterion
- 5:     let  $\Delta^{(k)} = 0$
- 6:     **while**  $\nabla^2 \mathcal{L}_B(\mathbf{x}^{(k)}) + \Delta^{(k)}$  is not positive definite **do**
- 7:       update  $\Delta^{(k)} := \max \left\{ 10^{-6} \mathbf{E}_n, 2\Delta^{(k)} \right\}$
- 8:     **end while**
- 9:     Cholesky decomposition according to (19)
- 10:     solve  $\mathbf{d}^{(k)}$  according to (18)
- 11:     update  $\mathbf{x}^{(k)}$  according to (17)
- 12:     **if** (20) holds **then**
- 13:       update  $\mathbf{x}^{(0)} = \mathbf{x}^{(k)}$
- 14:       break current loop
- 15:     **end if**
- 16:   **end while**
- 17:   update  $\mu := \theta\mu$
- 18: **end while**

---

that deviates from the optimal value of (13) by within  $m\theta^k \mu^{(0)}$ . Consequently, after precisely

$$\left\lceil \frac{\log(\epsilon/(m\mu^{(0)}))}{\log \theta} \right\rceil \quad (21)$$

solutions of (16), the algorithm can achieve the desired accuracy requirement of  $\epsilon$ . Next, we analyze the complexity required to solve (16), multiplying this by (21) gives the total complexity.

In each iteration, we need to calculate the iteration step size  $\alpha^{(k)}$  and the search direction  $\mathbf{d}^{(k)}$ , respectively. Here, the line search step to determine  $\alpha^{(k)}$  has a linear complexity. To determine  $\mathbf{d}^{(k)}$ , numerical methods (such as finite difference method) are used to calculate  $\nabla \mathcal{L}_B(\mathbf{x}^{(k)})$  and  $\nabla^2 \mathcal{L}_B(\mathbf{x}^{(k)})$ , with corresponding complexities of  $O(n)$  and  $O(n^2)$ , respectively. Directly attempting a Cholesky decomposition of the Hessian matrix has complexity of  $O(n^3)$ . Incorporating the above analysis, the overall computational complexity required for each iteration is  $O(n^3)$ .

In general, the number of iterations required to solve (14) using the Newton-like method is independent of the problem dimension  $n$  and typically ranges from about 10 to 20 [11]. In practice, the number of iterations is more dependent on the initial point, denoted as  $\gamma(\mathbf{x}^{(0)})$ . This is because the algorithm exhibits quadratic convergence near the convergence point, whereas if the initial point is far away, it may require more iterations to enter the rapidly converging region [11].

Ignoring the impact of initial point selection and parameter tuning, the computational complexity of solving the general nonconvex optimization problem (13) using the LMLB algorithm is  $O(n^3 \log m)$ , where  $n$  is the dimension of the problem and  $m$  represents the number of inequality constraints.

In the power allocation problem (12), if  $K = L \gg M = N$ , the computational complexity can be expressed as  $O((KM)^3 \log K)$ , the computational load of the algorithm

grows with the number of users  $K$  as  $K^3 \log K$ , and with the number of base station antennas  $M$  as  $M^3$ .

For heuristic algorithms SA and PSO, let the number of iterations be denoted as  $\gamma^{\text{SA}}$  and  $\gamma^{\text{PSO}}$ , respectively. In each iteration, the objective function and constraints must be evaluated, with an assumed complexity of  $O(n + nm)$ . In SA, let the number of inner loop iterations per iteration be denoted as  $\gamma_0$ , thus the overall complexity becomes  $O(\gamma^{\text{SA}} \cdot \gamma_0 \cdot nm)$ . For PSO, let the number of particles be denoted as  $Q$ , and the overall complexity is  $O(\gamma^{\text{PSO}} \cdot Q \cdot nm)$ .

Combining the previous discussion, heuristic algorithms have linear complexity, which is significantly better than LMLB, but they require more iterations and involve a larger number of parameters that need empirical tuning. LMLB is more computationally efficient for smaller problem dimensions, but heuristic algorithms are preferable for larger ones due to LMLB's cubic complexity increase with dimension.

#### IV. SIMULATION RESULTS AND DISCUSSIONS

In this section, we verify the effectiveness of our proposed algorithm through simulation. We set the location of MBS at  $(0, 0)$  with a radius of 500m and SBS at  $(600, 0)$  with a radius of 100m. It is assumed that all users are randomly and independently distributed in their respective cell. The specific simulation parameters are shown in Table I.

TABLE I  
SIMULATION PARAMETERS

Parameters	Value
$B_k, B_l/\text{MHz}$	10, 5
$\sigma^2/\text{dBm/Hz}$	-174
$P_{l,\max}^{\text{UL}}/\text{W}$	3
$P_{\max}^{\text{DL}}/\text{W}$	10
M, N	4
K, L	8

Fig. 2 depicts the system sum rate and Lagrangian function trends with the LMLB algorithm. The right-hand side vertical axis shows the convergence gap on a logarithmic scale. The figure also shows that smaller  $\mu$  requires more iterations for convergence and results in a smaller gap. However, excessively small  $\mu$  increases the gap due to the barrier term's reduced weight in  $\mathcal{L}_B$ , causing the iterative sequence to approach  $\mathbb{S}$  boundary.

Fig. 3 compares the system sum rate for varying user numbers with the baseline CLI mitigation scheme from [12], which uses Lagrange multipliers for power allocation. This scheme outperforms SA and PSO but falls short of LMLB. At lower dimensions, algorithmic differences are negligible, yet as the problem dimensionality rises linearly with the number of users, heuristic algorithms' effectiveness diminishes exponentially relative to LMLB due to the expanding solution space.

Fig. 4 shows the variations of two MUEs DL rate and two SUEs UL rate, as well as the average MUEs DL rate. The DL rate increases while the UL rate decreases, aligning with

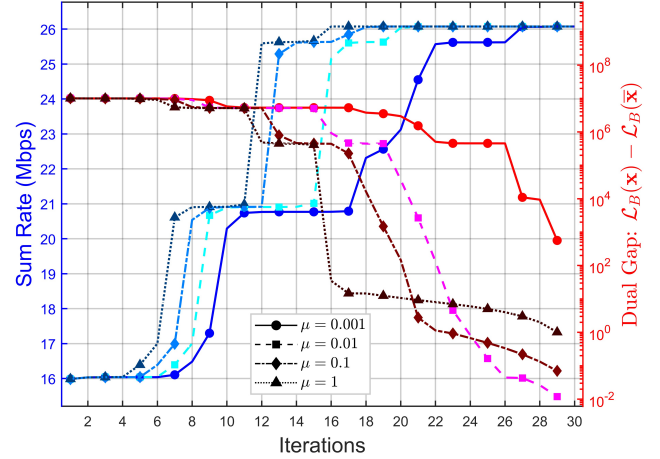


Fig. 2. Sum rate and  $\mathcal{L}_B$  under different values of  $\mu$  while using LMLB.

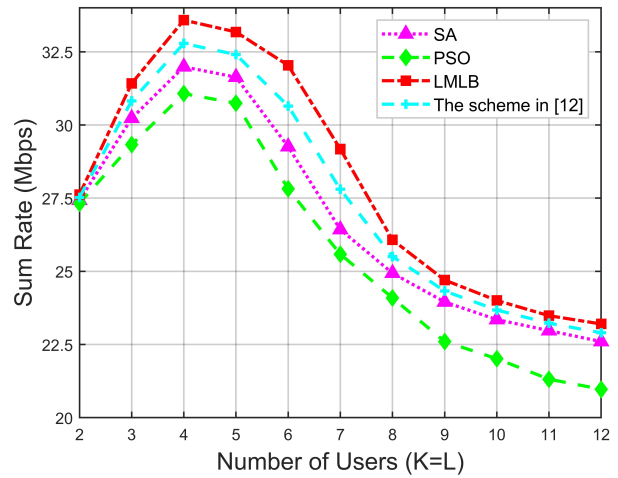


Fig. 3. Sum rate comparison for four algorithms ( $K=L$ ) under varying user numbers.

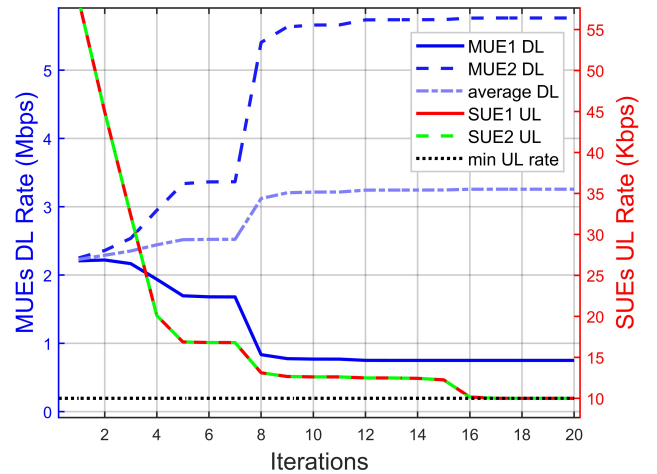


Fig. 4. The variations of individual MUEs' DL rate and individual SUEs' UL rate, as well as the average MUEs' DL rate under different number of iterations in LMLB.

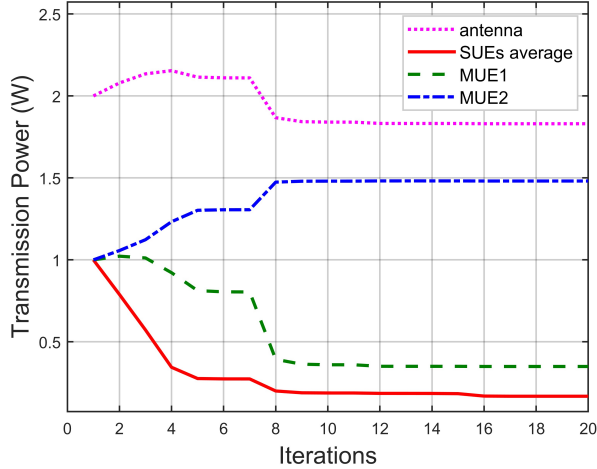


Fig. 5. The transmission power trends for an MBS antenna and the individual MUEs on the DL, as well as the average UL transmission power of SUEs under different number of iterations in LMLB.

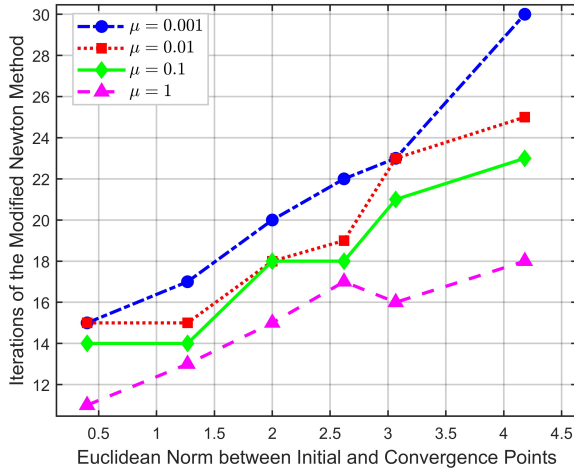


Fig. 6. The number of iterations required by the modified Newton descent method under various initial points configurations and different values of  $\mu$ .

theoretical expectations. The DL rate significantly exceeds the UL rate, making it the dominant factor in maximizing the overall system rate. Enhancing the DL rate requires boosting MBS transmission power, but this intensifies CLI for SBS, adversely affecting the UL rate. This effect is reciprocal in the small cell.

Fig. 5 illustrates the transmission power trends for an MBS antenna and the individual MUEs on the DL, as well as the average UL transmission power of SUEs. The figure shows a gradual decrease of UL power, aligning with theoretical analysis. Despite the DL rate’s significant role in optimization, higher DL transmission power is not always beneficial due to increased CLI and its potential to reduce the overall transmission rate of the system.

Fig. 6 shows the convergence behavior of the modified Newton descent method with respect to different initial points

and  $\mu$ . The figure indicates that in general a greater distance to the convergence point and a smaller  $\mu$  lead to an increased number of iterations, with extremely distant starting points potentially preventing convergence. A smaller  $\mu$  tightens the approximation to the optimum, diminishes the barrier term’s influence in  $\mathcal{L}_B$ , and enables closer approaches to the  $\mathbb{S}$  boundary, thus increasing iterations due to smaller steps.

## V. CONCLUSIONS

In this paper, we have proposed the LMLB algorithm to address power allocation problem in D-TDD based heterogeneous network comprising MBSs that transmit signals on the DL and SBSs that receive signals on the UL simultaneously. Our objective is to maximize the DL-UL total sum rate. The LMLB algorithm’s convergence, complexity, and performance relative to SA and PSO are evaluated, with simulations indicating a significant sum rate improvement. Theoretical analysis reveals a conflicting relation between system performance and interference mitigation. Reducing transmission power can alleviate the CLI while also potentially decreasing the system’s rate. Simulation results corroborate this finding. Additionally, the simulation experiments demonstrate that the convergence speed of LMLB is sensitive to initial conditions: a more appropriate configuration of initial values contributes to faster convergence.

## REFERENCES

- [1] H. Kim, J. Kim, and D. Hong, “Dynamic TDD systems for 5G and beyond: A survey of cross-link interference mitigation,” *IEEE Communications Surveys & Tutorials*, vol. 22, no. 4, pp. 2315–2348, 4th Quarter, 2020.
- [2] R1-1701613, “Overview of duplexing and cross-link interference mitigation,” *3GPP TSG RAN WG1 Meeting #88*, Feb. 2017.
- [3] R1-1701618, “Discussion on NR-LTE co-existence,” *3GPP TSG RAN WG1 Meeting #88*, Feb. 2017.
- [4] M. E. Benson et al., “Heterogeneous cyber-physical network coexistence through interference contribution rate and uplink power control algorithm (ICR-UPCA) in 6G edge cells,” *Internet of Things*, vol. 25, pp. 101031–101053, Apr. 2024.
- [5] H. Kim, K. Lee, H. Wang and D. Hong, “Cross link interference mitigation schemes in dynamic TDD systems,” in *Proc. VTC 2019-Fall*, Honolulu, HI, USA, Sep. 22-25, 2019, pp. 1–5.
- [6] K. Hiltunen and M. Matinmikko-Blue, “Interference control mechanism for 5G indoor micro operators utilizing dynamic TDD,” in *Proc. PIMRC 2018*, Bologna, Italy, Sep. 9-12, 2018, pp. 1–7.
- [7] K. Pedersen et al., “Advancements in 5G new radio TDD cross link interference mitigation,” *IEEE Wireless Communications*, vol. 28, no. 4, pp. 106–112, Aug. 2021.
- [8] K. Boutiba, M. Bagaa and A. Ksentini, “Multi-agent deep reinforcement learning to enable dynamic TDD in a multi-cell environment,” *IEEE Transactions on Mobile Computing*, vol. 23, no. 5, pp. 6163–6177, May 2024.
- [9] S. Hashempour, A. A. Suratgar, and A. Afshar, “Distributed nonconvex optimization for energy efficiency in mobile ad hoc networks,” *IEEE Systems Journal*, vol. 15, no. 4, pp. 5683–5693, Dec. 2021.
- [10] S. Boyd and L. Vandenberghe, *Convex Optimization*. Cambridge, U.K.: Cambridge University Press, 2004.
- [11] D. P. Bertsekas, *Nonlinear Programming (3rd ed.)*. Belmont, MA: Athena Scientific, 2016.
- [12] A. Lukowa and V. Venkatasubramanian, “Centralized UL/DL resource allocation for flexible TDD systems with interference cancellation,” *IEEE Transactions on Vehicular Technology*, vol. 68, no. 3, pp. 2443–2458, Mar. 2019.